Highly Reflective GaN-Based Air-Gap Distributed Bragg Reflectors Fabricated Using AlInN Wet Etching

Mathieu Bellanger[*], Valérie Bousquet, Gabriel Christmann[1], Jeremy Baumberg[1], and Matthias Kauer

Sharp Laboratories of Europe Ltd, Edmund Halley Road, Oxford Science Park, Oxford, OX4 4GB, U.K.
[1]*NanoPhotonics Centre, Cavendish Laboratory, University of Cambridge, Cambridge CB3 0HE, U.K.*

We report the fabrication of four-period GaN-based air-gap distributed Bragg reflectors (DBRs) using wet etching of sacrificial AlInN layers. The epitaxial structure grown by Molecular Beam Epitaxy consists of four GaN/$Al_{0.83}In_{0.17}N$ pairs. The sacrificial AlInN layers are selectively under-etched in hot nitric acid to form the air-gap DBR in micro-bridges. Micro-reflectivity spectra exhibiting flat and well defined stop-bands are observed, with peak reflectivities >99% at 590 nm and ∼74% at 400 nm. The full-width half maximum of the widest stop-band is 170 nm in agreement with transmission matrix simulations. Such devices are robust and offer an attractive basis for GaN-based microlasers and microcavities. © 2009 The Japan Society of Applied Physics

Monolithic distributed Bragg reflectors (DBRs) are used in III–nitride based optoelectronic devices to form cavities for vertical-cavity surface-emitting lasers (VCSELs)[1] and polariton lasers.[2] They can also be used to increase light extraction efficiency from light-emitting diodes (LEDs) or to shape their emission pattern.[3,4] Epitaxially grown III–nitride DBRs using Al_xGaN_{1-x}/ GaN[5,6] and AlInN/GaN[7] have been demonstrated, and reflectivities >99% have been achieved with both alloy combinations. However, due to the limited index contrast of these alloys, a large number of DBR periods are required for high DBR reflectivity using $Al_xGa_{1-x}N$/GaN or AlInN/GaN DBRs. While lattice-matched $Al_{0.83}In_{0.17}N$/GaN DBRs with >40 pairs can be grown without cracking or strain relaxation, the low index contrast ($\Delta n/n \sim 7\%$) results in a relatively small stop-band width of 30 nm for a 40-pair DBR.[4] The tolerances for DBR layer thickness and composition uniformity across the wafer are therefore small, otherwise undesirably large stop-band shifts will occur. On the other hand, air-gap DBRs can exhibit a similar reflectivity over a larger stop-band with only a few pairs.[3,8] Sharma *et al.* have reported a maximum reflectivity of ∼71% for a 4.5 pair air/$Al_{0.08}Ga_{0.92}N$ DBR fabricated using band-gap-selective photoelectrochemical etching.[3]

In this work, air-gap DBR structures were fabricated using wet etching of AlInN sacrificial layers in a hot nitric acid solution. Using $Al_{0.83}In_{0.17}N$, a lattice-matched DBR structure can be grown, and subsequently an uncomplicated wet etch can be used to selectively remove the AlInN layers to form the air-gaps. The etch selectivity with respect to the N-polar GaN face is good (∼500), leading to well defined air-gap DBR bridges.

A four-pair GaN/AlInN DBR, with respective thicknesses of $5\lambda/4 \times n_{GaN}$ (200 nm) and $\lambda/4 \times n_{air}$ (100 nm), designed for a center wavelength λ of 400 nm, was grown on a sapphire substrate (Fig. 1) with a V80 molecular beam epitaxy (MBE) system. Aluminum, gallium, indium elemental sources were used and elemental nitrogen was obtained from two different sources. In order to maintain suitable indium incorporation, the growth of the AlInN layers was performed at around 600 °C (growth rate ∼120 nm/h), the nitrogen gas being decomposed into active nitrogen atoms using a radio-frequency plasma source from
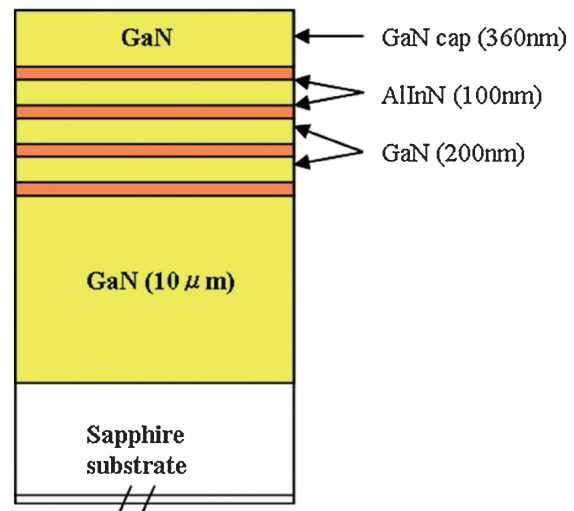
Fig. 1. Cross section of four-pair GaN/AlInN DBR sample grown by MBE.

Oxford Instruments. The GaN layers were grown at 900 °C (growth rate ∼500 nm/h) and nitrogen atoms were obtained from the thermal decomposition of ammonia gas. At the end of each DBR period growth, the substrate was removed from the growth chamber and X-ray diffraction as well as atomic force microscopy were performed to monitor lattice-matching and surface quality. Good AlInN/GaN interface quality is required to obtain smooth N-polar GaN surfaces after wet etching of the AlInN layers. The top surface roughness of the complete four-pair structure was measured by atomic force microscopy to be ∼1 nm (RMS) over a $4 \times 4\,\mu m^2$ area. A photolithography mask was then used to pattern micro-bridges of different length (L) and width (w) ($4 < L < 20\,\mu m$ and $2 < w < 20\,\mu m$), which were subsequently etched with an induced coupled plasma dry etch system using Ar and Cl_2 chemistry [Fig. 2(a)]. These dimensions, as well as the thickness of the cap layer (360 nm), were deduced from mechanical and force calculations that take into account micro-scale forces such as Van der Waals (VDW), capillary and elastic forces, as well as the buckling effect due to the built-in strain (S) within the air-gap structure. The attractive forces (VDW, capillary) were evaluated and compared to the elastic force for the structure in Fig. 1. It was concluded that a critical point drying

[*]E-mail address: mathieu.bellanger@sharp.co.uk
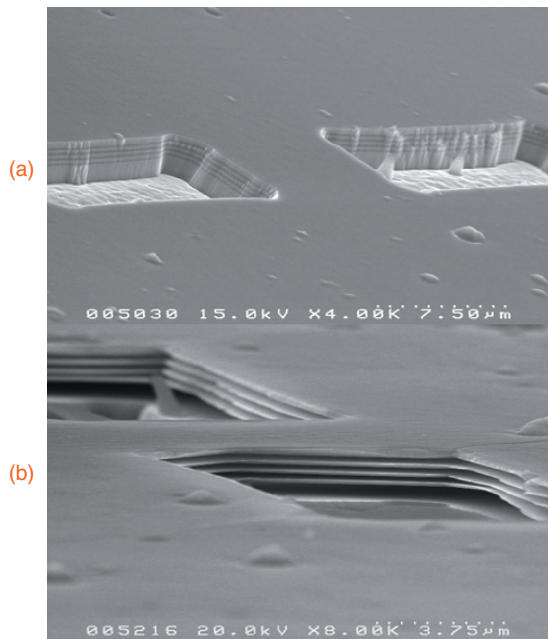
Fig. 2. Secondary electron microscopy (SEM) image of a four-period nitride air-gap DBR before (a) and after (b) 100 h etching in hot nitric acid. The dimensions of the micro-bridge are $10 \times 8 \, \mu m^2$.

Fig. 3. Micro-reflectivity set-up illuminated by xenon white light source. In the inset, the spot size (blue) is compared to the under-etched nanopipes.

method (CPD) should be used for structures with $L > 5 \, \mu m$ to avoid stiction of the suspended air-gap layers by capillary forces. The built-in strain (S) can be calculated with the difference between the thermal expansion coefficients ($\Delta \alpha = 1.9 \times 10^{-6} \, K^{-1}$) of GaN and sapphire substrate: $S = \Delta \alpha \times \Delta T \approx 1.9 \times 10^{-3}$ where ΔT is the difference in the growth temperature between these two materials ($\sim 1000 \, K$). The actual built-in strain was measured with X-ray diffraction and found to be 1.4×10^{-3}, slightly lower than predicted, possibly due to a partial release of the stress during the growth. Based on the Euler theory of beams,[9] the critical load is:

$$F_c = \frac{\pi^2 \times E \times I}{L^2} = A \times S \times E$$

with I being the area moment of inertia, E the Young modulus, and A the cross section area of a single micro-bridge. This corresponds to a critical buckling length L_c of $\sim 10 \, \mu m$, which was confirmed experimentally. Therefore the dimensions for the largest totally etched air-gap DBR micro-bridges were chosen to be $10 \times 8 \, \mu m^2$. These dimensions are small enough to maintain a good mechanical stability and large enough to be able to probe the micro-bridges during micro-reflectivity measurements.

The micro-bridges were under-etched in a 5 M hot nitric acid solution under reflux conditions.[10] Different acid concentrations between 2 and 10 M were tested and 5 M was found to be the best compromise between etching time and selectivity. The etching rate of AlInN in the 5 M HNO_3 solution was found to be $\sim 100 \, nm/h$ (~ 80 and $\sim 120 \, nm/h$ respectively for the 2 and 10 M solutions), and the etch selectivity to GaN ~ 500. A temperature controller was used to set the nitric acid solution temperature to $\sim 120 \, °C$, just below its boiling point, to accelerate the chemical reaction while inhibiting the formation of bubbles that could make
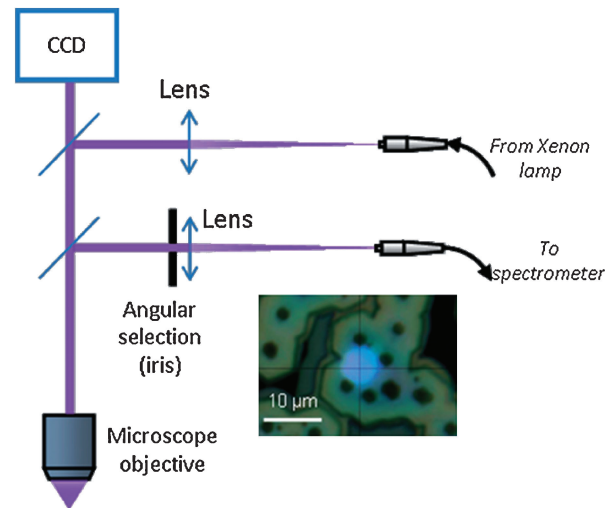
the air-gap structures collapse. After etching, the air-gap DBRs were dried by CPD with liquid CO_2 used as a medium fluid. The final air-gap DBR structure after 100 h of wet etching is shown in Fig. 2(b). The overall uniformity of the air-gap DBRs was good, although in some cases the exposed N-polar GaN surfaces were slightly etched at the edges of the micro-bridges in the growth direction. This can be explained by the finite selectivity of the etchant (~ 500) in the (0001) direction and the position-dependent difference in etching time perpendicular to the main axis of the micro-bridges, particularly for the smaller micro-bridges ($w < 5 \, \mu m$) which were over-etched for about 50 h.

Micro-reflectivity spectra were recorded between 350 and 800 nm on several four-pair micro-bridges. The set-up employed a xenon white light source relayed through a $200 \, \mu m$ core optical fiber imaged onto the sample using a $\times 100$ long working distance near-UV objective to a spot of diameter $\sim 8 \, \mu m$ (Fig. 3). The reflected light was collected off a beamsplitter and focused onto a second $200 \, \mu m$ optical fiber coupled to a UV spectrometer for analysis. An iris aperture coupled to a collimation lens was used to select the angular width of the reflected light to $\sim 5°$. An imaging charge coupled device (CCD) camera is installed on the setup, allowing simultaneous acquisition of sample images. The experimental results obtained on a $10 \times 8 \, \mu m^2$ air-gap DBR micro-bridge (red curve in Fig. 4) are in good agreement with our simulations based on transmission matrix (TM) simulations (black curve in Fig. 4). The reflectivity spectra show two stop-bands of high reflectivity centered at 400 nm ($\sim 74\%$ peak reflectivity) and 590 nm respectively ($> 99\%$ reflectivity), with widths of 50 and 170 nm, respectively. The presence of the two stop-bands is due to the higher-order optical thickness of the GaN layer ($5\lambda/4$) compared to the air layer, specifically chosen to reduce bending of the thin layers. The difference between theoretical ($> 99\%$) and experimental values for the peak reflectivity at 400 nm can be explained by observed air-gap DBR non-uniformity and by the slight etching of the GaN layers in the (0001) direction, as already discussed.
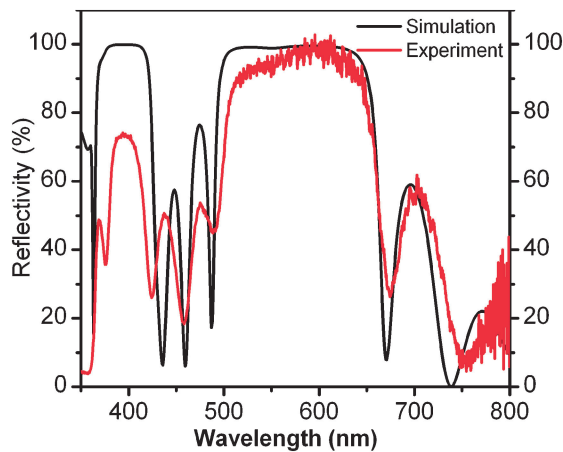
Fig. 4. Experimentally measured and simulated reflectivity spectra for a 10 x 8 µm² air-gap DBR micro-bridge.

A hot nitric acid solution was used with an etch rate of ∼100 nm/h. The thickness uniformity of the air-gap DBR was very good across the sample, resulting from high material quality and highly selective etching. Micro-reflectivity measurements performed on 10 × 8 µm² micro-bridges exhibited two wide stop bands of high reflectivity centered at 400 (∼74%) and 590 nm (>99%), in agreement with transmission matrix simulations. The maximum reflectivity of air-gap DBRs formed at nanopipes locations was found to be ∼95%. The demonstration of high reflectivity air-gap DBRs fabricated by an uncomplicated wet etching process creates new possibilities for the use of nitrides air-gap DBRs in short wavelength optoelectronic devices such as UV/blue VCSELs or LEDs.

Furthermore, it was found that the nitric acid penetrates into hexagonal defects identified as nanopipes[11] and under-etches the region around these defects producing additional air gap DBRs (Fig. 3. inset). Measurements performed in such areas result in similar high-reflectivity spectra with peak reflectivities >95% in the vicinity of most of these nanopipes. Moreover, the uniformity of the reflectivity across the sample (for both micro-bridges and nanopipes) was good with an average peak reflectivity of 90%. We believe that reducing the spot size would give an even higher peak reflectivity at 400 nm since it is likely that smaller air-gap DBR regions have a better homogeneity. Furthermore, air-gap DBR structures grown on free standing GaN substrates instead of sapphire are expected to have a higher reflectivity, since buckling effects due to the built-in strain will be avoided.

In conclusion, we have demonstrated the fabrication and characterization of high reflectivity four-pair GaN/air-gap DBRs grown by MBE. Selective etching of AlInN layers was performed to release the air-gap DBR micro-bridges.

1) T.-C. Lu, C.-C. Kao, H.-C. Kuo, G.-S. Huang, and S.-C. Wang: Appl. Phys. Lett. **92** (2008) 141102.
2) S. Christopoulos, G. Baldassarri Höger von Högersthal, A. J. D. Grundy, P. G. Lagoudakis, A. V. Kavokin, J. J. Baumberg, G. Christmann, R. Butté, E. Feltin, J.-F. Carlin, and N. Grandjean: Phys. Rev. Lett. **98** (2007) 126405.
3) R. Sharma, Y.-S. Choi, C.-F. Wang, A. David, C. Weisbuch, S. Nakamura, and E. L. Hu: Appl. Phys. Lett. **91** (2007) 211108.
4) J. Dorsaz, J.-F. Carlin, S. Gradecak, and M. Ilegems: J. Appl. Phys. **97** (2005) 084505.
5) H. M. Ng, T. D. Moustakas, and S. N. G. Chu: Appl. Phys. Lett. **76** (2000) 2818.
6) K. E. Waldrip, J. Han, J. J. Figiel, H. Zhou, E. Makarona, and A. V. Nurmikko: Appl. Phys. Lett. **78** (2001) 3205.
7) J.-F. Carlin, J. Dorsaz, E. Feltin, R. Butté, N. Grandjean, M. Ilegems, and M. Laügt: Appl. Phys. Lett. **86** (2005) 031107.
8) R. Sharma, E. D. Haberer, C. Meier, E. L. Hu, and S. Nakamura: Appl. Phys. Lett. **87** (2005) 051107.
9) W. Fang and J. A. Wickert: J. Micromech. Microeng. **4** (1994) 116.
10) I. M. Watson, C. Xiong, E. Gu, M. D. Dawson, F. Rizzi, K. Bejtka, P. R. Edwards, and R. W. Martin: Proc. SPIE **6993** (2008) 69930E.
11) S. K. Hong, B. J. Kim, H. S. Park, Y. Park, S. Y. Yoon, and T. I. Kim: J. Cryst. Growth **191** (1998) 275.